Structure and Photophysics of 2-(2′-Pyridyl)benzindoles: The Role of Intermolecular Hydrogen Bonds

Irina Petkova,[†,‡,£] Maria S. Mudadu,[§] Ajay Singh,[§] Randolph P. Thummel,*[,§] Ivo H. M. van Stokkum,[#] Wybren Jan Buma,*[,£] and Jacek Waluk*[,†]

Institute of Physical Chemistry, Polish Academy of Sciences, Kasprzaka 44/52, 01-224 Warsaw, Poland, Institute of Organic Chemistry, Bulgarian Academy of Sciences, Akad. G. Bontchev bl. IX, Sofia 1113, Bulgaria, Van't Hoff Institute for Molecular Sciences, University of Amsterdam, Nieuwe Achtergracht 166, 1018 WV Amsterdam, The Netherlands, Department of Chemistry, University of Houston, Houston, Texas, 77204-5003, and Faculty of Sciences, Vrije Universiteit, De Boelelaan 1081, 1081 HV Amsterdam, The Netherlands

Received: May 10, 2007; In Final Form: August 23, 2007

The photophysical properties of two isomeric 2-(2′-pyridyl)benzindoles depend on the environment. Strong fluorescence is detected in nonpolar and polar aprotic solvents. In the presence of alcohols, the emission reveals an unusual behavior. Upon titration of *n*-hexane solutions with ethanol, the fluorescence intensity goes through a minimum and then increases with rising alcohol concentration. Transient absorption and time-resolved emission studies combined with ground- and excited-state geometry optimizations lead to the conclusion that two rotameric forms, *syn* and *anti*, coexist in alcohols, whereas in nonpolar and aprotic polar media, only the *syn* conformation is present. The latter can form cyclic complexes with alcohols, which are rapidly depopulated in the excited state. In the presence of excess alcohol, *syn* → *anti* rotamerization occurs in the ground state, promoted by the cooperative action of nonspecific and specific effects such as solvent polarity increase and the formation of hydrogen bonds to both donor and acceptor sites of the bifunctional compounds.

1. Introduction

Hydrogen bonding can exert a profound effect on the processes responsible for the deactivation of excited electronic states.[1−36] One of the fundamental photochemical reactions, excited-state proton transfer (ESPT),[24,37−39] usually occurs along a hydrogen bond, intra- or intermolecular. The former is possible in bifunctional molecules, simultaneously possessing proton donor and acceptor groups. ESPT has been extensively investigated, not only because it involves a quantum mechanical process that is yet to be fully understood but also because it is a ubiquitous phenomenon which influences the dynamic behavior of a wide variety of systems. Knowledge of the fundamental laws of proton-transfer reactions in homogeneous media, as well as in organized molecular systems, is necessary to understand the mechanisms of natural proton transport and to design model and artificial molecular devices. Investigations of excited-state proton-transfer reactions can provide important information on the local structure and dynamics of biological systems. Among such systems, the photoreaction of DNA is of great interest because of its implications in radiation-induced mutations or carcinogenesis resulting from the possible involvement of rare tautomeric enol forms of the bases during DNA replication.[40,41] Tautomerization in DNA still has not been well characterized experimentally because, in addition to the difficulties inherent in studying the ultrafast and reversible proton transfer, it has not been possible to selectively initiate proton transfer within a specific base pair. However, the ESPT reaction in a model for DNA base pairs, the 7-azaindole dimer (7AI), has been studied extensively.[42−69] In this chromophore, two protons are transferred upon photoexcitation. Whether the process occurs in a stepwise or synchronous fashion has been a matter of strong controversy.[58,59,62−64,69] Phototautomerization has also been discovered in complexes of 7AI with alcohols and water.[70−84]

We have been carrying out detailed studies of bifunctional chromophores based on indole, pyrrole, pyridine, and carbazole units, such as 2-(2′-pyridyl)indoles,[4,5,8,13,18,20,21,31] 2-(2′-pyridyl)-pyrrole,[32,85] 7-(pyridyl)indoles,[35] dipyrido[2,3-*a*:3′,2′-*i*]carbazole,[10,22,25] 7,8,9,10-tetrahydro-11*H*-pyrido[2,3-*a*]carbazole,[18,22] or 1*H*-pyrrolo[3,2-*h*]quinoline.[19,21,22,27,31,86] These molecules, structurally similar to 7AI, differ in the number of bonds between the proton donor (the NH group) and the acceptor (pyridine-type nitrogen). The basic and acidic sites are separated by two bonds in 7AI and by three bonds in our compounds. This difference has a crucial impact on the photophysics; ESPT in alcohols is accelerated by about 2 orders of magnitude with respect to 7AI. This acceleration is due to much stronger, compared to 7AI, double intermolecular hydrogen bonds in cyclic 1:1 complexes with alcohols or water. On the contrary, the hydrogen bonds in the 7AI dimer are more linear and stronger than those in our compounds. As a consequence, no phototautomerization was observed for our chromophores in their dimeric forms.[25]

In addition to ESPT, our compounds reveal efficient fluorescence quenching by alcohols and by azaaromatic proton acceptors, such as pyridine or quinoline.[5,26] Finally, for molecules with separate moieties containing proton donor and

[†] Polish Academy of Sciences.
[‡] Bulgarian Academy of Sciences.
[£] University of Amsterdam.
[§] University of Houston, Houston.
[#] Vrije Universiteit.

10.1021/jp0735841 CCC: $37.00
Published on Web 10/13/2007

CHART 1

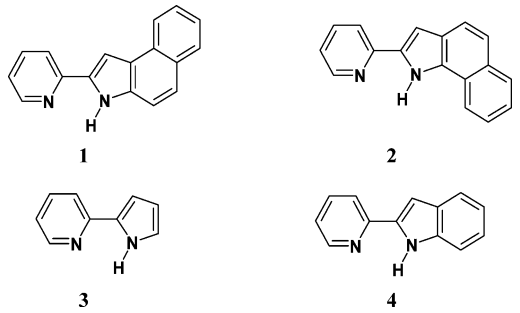

acceptor groups linked by a single bond, such as 2-(2′-pyridyl)-indole and 2-(2′-pyridyl)pyrrole, we observed alcohol-induced *syn*−*anti* rotamerization in the ground state.[20,32] The *syn* structures, with both nitrogen atoms on the same side of the molecule, are more stable in nonpolar and polar aprotic solvents, whereas in alcohols, the energy ordering is reversed, and the *anti* forms become dominant. Two factors are responsible for the *syn*−*anti* equilibrium shift. First, the dipole moments are larger for the *anti* forms, which favors these structures in polar solvents. Second, formation of separate hydrogen bonds with two molecules of alcohol in the *anti* structure is energetically more favorable than hydrogen bonding in the *syn* species. These two effects, nonspecific and specific solvation, add up, making the *anti* forms dominant in polar, protic alcohols, but not in polar, nonprotic solvents, such as acetonitrile.

The nonspecific solvation by polar solvents should be more efficient for smaller chromophores due to a smaller Onsager cavity radius. Indeed, we observed that for 2-(2′-pyridyl)pyrrole (PP), traces of the *anti* form could be observed in acetonitrile,[32] whereas for the larger 2-(2′-pyridyl)indole (PyIn-0), this form could only be detected in alcohols.[20]

In order to find out whether a further increase in molecular size can reduce the effect of nonspecific solvation, this work examined two isomeric molecules closely related to PP and PyIn-0. These molecules were 2-(2′-pyridyl)benz[*e*]indole (**1**) and 2-(2′-pyridyl)benz[*g*]indole (**2**), bifunctional compounds possessing both a proton donor and acceptor in the same arrangement as PP (**3**) and PyIn-0 (**4**) (Chart 1). In studying the *syn*−*anti* equilibrium, we made use of the fact that a *syn* conformer can bind an alcohol molecule in a cyclic fashion, whereas an *anti* structure cannot. Therefore, the observation of phototautomerization in the presence of alcohols is a strong indication of the existence of the *syn* form.

Our experimental results are complemented by theoretical studies of conformational and tautomeric structures in both S_0 and S_1 electronic states. The results show that the general tendency of the *syn*−*anti* equilibrium being shifted toward the *anti* form in alcohols is preserved in **1** and **2**. However, contrary to the case of smaller molecules, significant fractions of the *syn* species were detected in alcohol solutions of both **1** and **2**, indicating that conformational equilibria can be controlled by a careful choice of molecular size and the properties of the environment.

2. Experimental and Computational Details

The pyridyl-substituted benzindoles were prepared by implementation of the Fisher indole synthesis. The condensation of 1- or 2-naphthylhydrazine with 2-acetylpyridine led to the corresponding hydrazones in high yields. The hydrazone was then heated with zinc chloride in acetic acid to afford the cyclized indole product. The 1-naphthylhydrazone **2p** can lead only to the benz[*g*]indole (**2**) by cyclization at the naphthalene 2-position. The 2-naphthylhydrazone **1p**, on the other hand, can cyclize at either the naphthalene 1 or 3 position. Reaction occurs preferentially at the 1 position to provide the benz[*e*]indole (**1**), albeit in modest yield.[87]

SCHEME 1

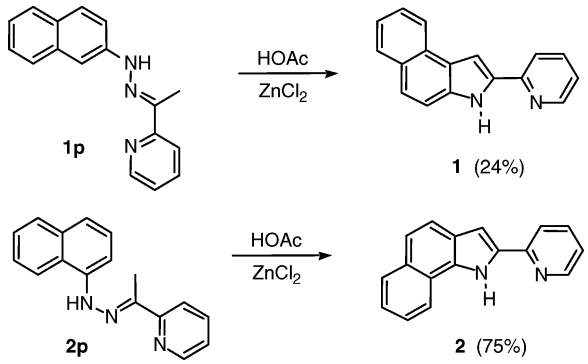

Nuclear magnetic resonance spectra were recorded on a General Electric QE-300 spectrometer at 300 MHz for ^{1}H and 75 MHz for ^{13}C, referenced to DMSO-d_6, and TMS in $CDCl_3$. Melting points were recorded on a Thomas Hoover capillary melting point apparatus, and they were uncorrected. All of the reagents were commercially available. Elemental analyses were performed by QTI, Inc., Whitehouse, NJ.

2.1. 2-Naphthylhydrazone of 2-Acetylpyridine (1p). A mixture of 2-naphthylhydrazine hydrochloride (2.34 g, 12.0 mmol), 2-acetylpyridine (1.21 g, 10.0 mol), and glacial HOAc (4 drops) in absolute EtOH (30 mL) was refluxed for 5 h. After cooling to room temperature, the precipitate was filtered to provide **1p** as a bright-orange solid (2.50 g, 96%): mp 263−265 °C; ^{1}H NMR (DMSO-d_6) δ 10.54 (s, 1H), 8.76 (d, 1H, J = 5.1 Hz), 8.41 (t, 1H, J = 7.8 Hz), 8.31 (d, 1H, J = 8.1 Hz), 8.01(s, 1H), 7.73−7.86 (overlapping m, 5H), 7.45 (td, 1H, J = 6.9, 0.9 Hz), 7.31 (d, 3H, J = 7.8 Hz), 2.51 (s, 3H).

2.2. 1-Naphthylhydrazone of 2-Acetylpyridine (2p). In the manner described for **1p**, a mixture of 1-naphthylhydrazine hydrochloride (2.34 g, 12.0 mmol), 2-acetylpyridine (1.21 g, 10.0 mol), and glacial HOAc (4 drops) in absolute EtOH (14 mL) provided **2p** as an orange solid (1.16 g, 95%): mp 243−246 °C; ^{1}H NMR (DMSO-d_6) δ 9.88 (s, 1H), 8.70 (d, 1H, J = 5.4 Hz), 8.34 (overlapping m, 3H), 7.85−7.94 (overlapping m, 2H), 7.71 (m, 1H), 7.48−7.59 (overlapping m, 4H), 2.58 (s, 3H).

2.3. 2-(2′-Pyridyl)benz[*e*]indole (1). A mixture of **1p** (0.78 g, 3.0 mmol) and $ZnCl_2$ (1.63 g, 12.0 mmol) in glacial HOAc (50 mL) was refluxed for 4 days to provide a precipitate, which was collected and purified by chromatography on silica gel, eluting with EtOAc/CH_2Cl_2 (8:2). Recrystallization from CH_2Cl_2/hexane provided **1** as a white solid (0.18 g, 24%): mp 121−122 °C; ^{1}H NMR (DMSO-d_6) δ 12.11 (s, 1H), 8.63 (d, 1H, J = 5.1 Hz), 8.28 (d, 1H, J = 8.1 Hz), 8.03 (d, 1H, J = 7.8 Hz), 7.85−7.92 (overlapping m, 2H), 7.81 (d, 1H, J = 2.1 Hz), 7.65 (d, 1H, J = 8.7 Hz), 7.58 (d, 1H, J = 9.3 Hz), 7.55 (t, 1H, J = 7.8 Hz), 7.40 (t, 1H, J = 8.1 Hz), 7.28 (dd, 1H, J = 6.0, 0.9 Hz); ^{13}C NMR ($CDCl_3$) δ 150.4, 149.0, 137.1, 134.8, 133.7, 129.6, 128.9, 128.5, 126.2, 124.7, 124.4, 123.8, 123.0, 121.8, 119.8, 113.2, 100.4. Anal. Calcd for $C_{17}H_{12}N_2$: C, 83.61; H, 4.92; N, 11.47. Found: C, 83.55; H, 4.84; N, 11.41.

2.4. 2-(2′-Pyridyl)benz[*g*]indole (2). A mixture of **2p** (1.04 g, 4.0 mmol) and $ZnCl_2$ (1.09 g, 8.0 mmol) in glacial HOAc (50 mL) was refluxed under Ar for 48 h to provide a precipitate.

Chromatography on silica gel, eluting with EtOAc, gave a solid, which was recrystallized from benzene to provide **2** (0.75 g, 75%): mp 155−157 °C; ^{1}H NMR (DMSO-d_6) δ 12.45 (s, 1H), 8.82 (d, 1H, J = 8.1 Hz), 8.66 (d, 1H, J = 5.1 Hz), 8.04 (d, 1H, J = 8.1 Hz), 7.85−7.93 (overlapping m, 2H), 7.68 (d, 1H, J = 8.7 Hz), 7.28−7.56 (overlapping m, 5H); ^{13}C NMR ($CDCl_3$) δ 150.5, 149.0, 137.1, 135.0, 131.9, 131.3, 129.1, 125.9, 125.4, 124.7, 122.1, 121.8, 121.5, 121.0, 120.4, 119.7, 102.6. Anal. Calcd for $C_{17}H_{12}N_2$: C, 83.61; H, 4.92; N, 11.47. Found: C, 83.38; H, 4.83; N, 11.35.

Electronic absorption spectra were measured on a Shimadzu UV 3100 spectrophotometer and a HP 8453 diode array spectrometer. Stationary fluorescence spectra were recorded and corrected for the instrumental response using either an Edinburgh FS 900 CDT or a Spex Fluorolog 3 spectrofluorimeter. For the determination of quantum yields, quinine sulfate in 0.1 N H_2SO_4 was used as a standard (Q_{fl} = 0.51[88]). The solvents, *n*-hexane, acetonitrile (Aldrich), methanol, propanol-1, butanol-1 (Merck), and ethanol (Chempur, Aldrich), were checked for the presence of fluorescent impurities.

Fluorescence lifetimes were measured on an Edinburgh FL 900 CDT time-resolved fluorimeter (estimated resolution: 0.2−0.3 ns) using a time-correlated single-photon counting technique. Time-resolved fluorescence was measured using a picosecond time-correlated single-photon counting setup described in detail before.[89] Excitation was provided by a mode-locked argon ion laser (Coherent 486 AS Mode Locker and Coherent Innova 200 laser), which synchronously pumped a dye laser (Coherent model 700) operating on DCM. The dye laser, frequency-doubled with a BBO crystal, yielded 310−320 nm pulses. A Hamamatsu microchannel plate photomultiplier (R3809) was used as the detector. The response function of the instrument had a fwhm of ≈17 ps.

The setup used for the femtosecond transient absorption experiments closely followed the one described before.[90] Briefly, a 130 fs (fwhm) pulse train at 800 nm with a repetition rate of 1 kHz was generated by a Spectra Physics Hurricane regenerative amplifier laser system and was separated into two parts. One part pumped a Spectra Physics OPA 800 system to provide excitation pulses; the other part was focused on a calcium fluoride crystal to generate a white-light continuum, from ∼350 to ∼800 nm, used for the probe pulse. The total instrumental response was about 200 fs (fwhm). In the present experiments, magic angle conditions were used for the pump and probe beams. Experiments were performed at ambient temperature on solutions with an optical density of ∼0.5 in a 1 mm cell. To avoid effects resulting from the high transient power radiation, the excitation power was kept as low as ∼5 μJ/pulse using a pump spot diameter of about 1 mm. Apart from lowering the excitation intensity, the influence of thermal effects and the possible photodegradation of the sample was taken care of by placing the circular cuvette containing the solution in a homemade rotating ball bearing (1000 rpm). Absorption and emission spectra taken under these conditions before and after the experiments were indeed identical.

Density functional calculations were performed using the TURBOMOLE 5.7 suite of programs.[91−94] The calculations used a Gaussian AO basis set of triple-ζ quality augmented with polarization functions (*def*-TZVP[95]), the hybrid B3LYP functional,[96,97] a large grid for numerical quadrature ("grid m3" option), and convergence of the ground-state energy and density matrix to at least 10^{-8} au. The geometry of the molecule in the ground and excited states was optimized using analytical DFT and TD-DFT[98] gradients, respectively. At the equilibrium geometries, harmonic force fields were calculated using numerical (two-side) differentiation of the gradients for both the ground and excited states.

TABLE 1: Results of Calculation of Excited-State Energies and Dipole Moments for the *syn* Form of 1

Calculated at Optimized S_0 Geometry			
state	energy in cm^{-1} (nm)	dipole moment (D)	oscillator strength
S_0 (1 ^{1}A′)	0	2.3	
2 ^{1}A′	28320 (353)	4.4	0.67
3 ^{1}A′	30712 (326)	6.4	0.009
4 ^{1}A′	31506 (317)	6.9	0.03
5 ^{1}A′	33428 (299)	3.0	0.03
6 ^{1}A′	36056 (297)	2.2	0.04
1 ^{1}A″	38350 (261)	5.7	0.0015

Calculated at Optimized S_i Geometry			
state S_i	$\Delta E(S_i - S_0)$ (nm)	dipole moment S_i (D)	dipole moment S_0 (D)
2 ^{1}A′	25950 (385)	4.2	2.4
3 ^{1}A′	a	a	a
4 ^{1}A′	29951 (334)	5.2	2.6

[a] No convergence could be achieved.

TABLE 2: Results of Calculation of Excited-State Energies and Dipole Moments for the *syn* Form of 2

Calculated at Optimized S_0 Geometry			
state	energy in cm^{-1} (nm)	dipole moment (D)	oscillator strength
S_0 (1 ^{1}A′)	0	2.3	
2 ^{1}A′	28649 (349)	5.7	0.36
3 ^{1}A′	30222 (330)	2.7	0.17
4 ^{1}A′	32041 (312)	9.5	0.12
5 ^{1}A′	33079 (302)	3.3	0.11
6 ^{1}A′	34862 (287)	5.0	0.27
1 ^{1}A″	38497 (260)	4.9	0.015

Calculated at Optimized S_i Geometry			
state S_i	$\Delta E(S_i - S_0)$ (nm)	dipole moment S_i (D)	dipole moment S_0 (D)
2 ^{1}A′	25443 (393)	7.7	2.8
3 ^{1}A′	27786 (360)	4.6	2.5
4 ^{1}A′	29431 (339)	6.8	2.6

3. Results and Discussion

3.1. Calculations. Because of the presence of a single bond connecting the pyridyl and benzindole moieties, **1** and **2** can exist in two planar conformations, either the *syn* or *anti* rotameric form. Their relative energies can be influenced by both specific effects (hydrogen bond formation) and nonspecific interactions with the solvent. We performed ground- and excited-state geometry optimizations to examine the relative energies of the two forms. The calculated electronic transition energies and dipole moments are presented for the most stable *syn* form of **1** and **2** in Tables 1 and 2, respectively. Figure 1 presents a scheme of relative energies of various rotameric and tautomeric species of **2** (the results for **1** are very similar).

The ground-state calculations predict that for both compounds, the *syn* form is more stable than the *anti* species by about 4.7 kcal/mol. Very similar energy differences between the *syn* and *anti* forms have been calculated previously for **3**[32] and **4**[20]. The dipole moment in the ground state of the *anti* form is larger than that of the *syn* form; for **1**, $\mu(syn)$ = 2.3 D and $\mu(anti)$ = 3.5 D. The corresponding values for **2** are 2.3 and 3.1 D, respectively, and analogous results were obtained for **3** (1.1 and

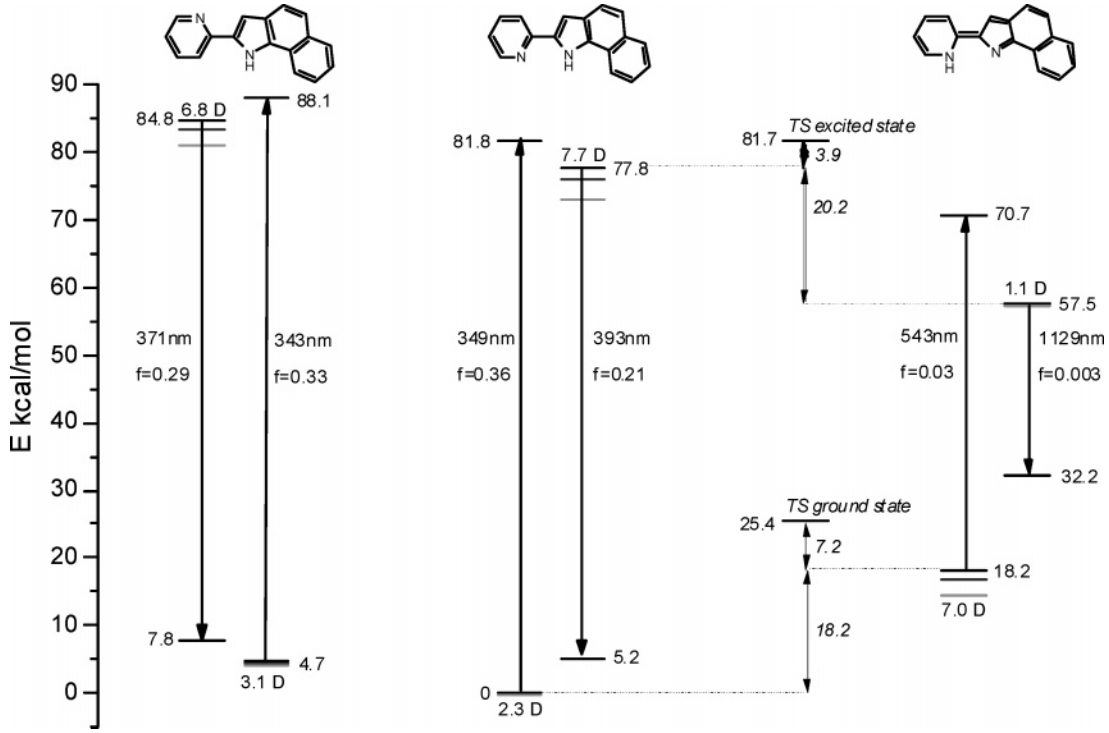

Figure 1. The diagram of calculated energy levels, transition energies, oscillator strengths, and dipole moments for 2-(2′-pyridyl)benz[*g*]indole (**2**). Black, dark gray, and light gray lines indicate energies calculated for the gas phase, nonpolar (*n*-hexane), and polar media (methanol), respectively; arrows indicate absorption and fluorescence FC transitions. The dipole moments are given for the optimized structures.

3.2 D) and **4** (2.4 and 3.4 D). These findings lead to a general prediction that in nonpolar media, the *syn* conformers should be dominant, but the *anti*−*syn* energy difference should decrease with increasing solvent polarity. The simple Onsager model expression can be applied to estimate the solvation energy

$$E_{\mathrm{solv}} = -\frac{\mu^2}{4\pi\epsilon_0 a^3}\left(\frac{\epsilon - 1}{2\epsilon + 1}\right)$$

where μ, ϵ, and a are the dipole moment, the dielectric constant, and the Onsager cavity radius, respectively. Assuming $a \approx 5$ Å, for the ground state of **2** in methanol, one finds a small decrease of ΔE_{as}, the *anti*−*syn* energy difference, by 0.24 kcal/mol with respect to vacuum. One can safely conclude that the increase of solvent polarity is not able to change the *syn*−*anti* energy ordering. The same is true for the lowest calculated excited singlet state, for which the dipole moment in the optimized *syn* form is 7.7 D, compared to 6.8 D in the *anti* structure. The ΔE_{as} value calculated for S_1 of **2** is 7.0 kcal/mol in *n*-hexane; it increases to 7.7 kcal/mol when the dielectric constant of methanol is used. Thus, the calculations predict that the *syn* form should be dominant both in nonpolar and polar media in S_0 as well as in S_1.

The above scheme does not take into account the possibility of additional stabilization of the *anti* form resulting from the formation of intermolecular hydrogen bonds with protic solvents, especially those that can simultaneously act as proton donors and acceptors. It has been demonstrated for **3**[32] and **4**[20] that the *anti* form is dominant in bulk alcohols because two strong, linear hydrogen bonds with two different alcohol molecules, possible for this form, are energetically more favorable than the hydrogen bond arrangement in the complexed *syn* species.

For both compounds, the calculations predict several $\pi\pi^*$ transitions in the low-energy region. On the other hand, the expected absorption intensity patterns should be very different; for **1**, only one strong transition is predicted, while for **2**, the calculations reveal five transitions of comparable intensity in the region between 28 600 and 34 900 cm^{-1}. These different patterns are indeed observed in the experimental spectra (Figures 2 and 3).

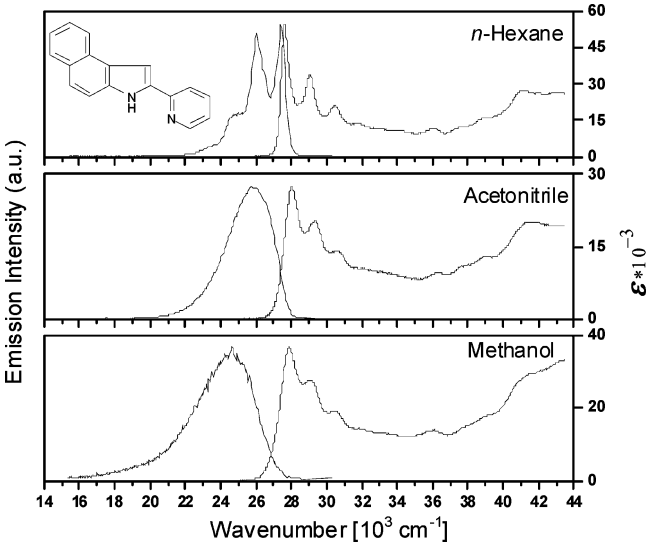

Figure 2. Room-temperature absorption and fluorescence of **1** in *n*-hexane, acetonitrile, and methanol.

For both molecules in the $\pi\pi^*$ excited singlet states, another possible structure should be considered. The electron density redistribution occurring upon excitation may provide a driving force for the excited-state proton transfer. The redistribution leads to an increase in the excited-state pK_a for the proton acceptor, a decrease in the excited-state pK_a for the proton donor, or a combination of both. Large changes of both pK_a values have been reported for **3**, **4**, and other structurally similar molecules.[8,19,20,32,35] One can thus expect that a phototautomer, with the proton attached to the pyridine nitrogen, can become the lowest-energy form in S_1. The calculations firmly confirm

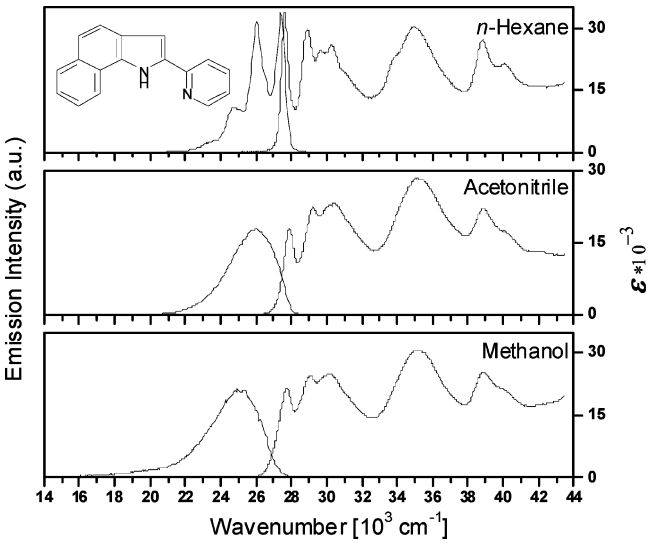

Figure 3. Room-temperature absorption and fluorescence of **2** in *n*-hexane, acetonitrile, and methanol.

this prediction. Proton transfer in S_1 in the *syn* form of **2** results in the phototautomer lying 20.2 kcal/mol lower. This difference is about the same in magnitude but opposite in sign as the energy separation between the normal and tautomeric *syn* forms in the ground state, 18.2 kcal/mol. The barriers to proton transfer were calculated to be 3.9 kcal/mol in S_1 and 7.2 kcal/mol for the back reaction in S_0. Thus, ESPT is possible thermodynamically, but the barrier is rather substantial. It can be largely reduced, however, in a cyclic 1:1 complex with water or alcohol.[99]

Interestingly, the calculations show that a Franck−Condon vertical transition excites the molecule slightly above the barrier for the proton transfer. One could envisage tautomerization to occur if the proton-transfer rate is faster or comparable to that of vibrational relaxation. Actually, such a reaction from an unrelaxed excited molecule seems to be occurring in **3**.[100]

In summary, the computations predict that the *syn* forms should be more stable in nonpolar and polar aprotic solvents, but the situation may change in protic environments. ESPT is thermodynamically favorable, but kinetically improbable, unless the barrier can be lowered by forming a cyclic complex with alcohol.

These theoretical predictions will now be compared with the experimental data.

3.2. Stationary Absorption and Fluorescence. Room-temperature absorption and fluorescence spectra recorded for three different types of solvents, nonpolar *n*-hexane, polar aprotic acetonitrile, and polar and protic methanol, are shown in Figures 2 and 3 for **1** and **2**, respectively. The absorption intensity patterns of the first few electronic transitions are quite different for the two molecules and quite nicely reproduced by calculations (Tables 1 and 2). In both compounds, the lowest transition lies at practically the same energy (~27 600 cm^{-1} in *n*-hexane) and reveals a very similar vibronic structure. In acetonitrile, this transition is slightly shifted to the blue. In methanol, it shifts back to the red, which suggests that hydrogen bonding interactions with the solvent are stronger in the excited state. The blue shift in polar solvents is often an indication that the dipole moment decreases in the excited state. However, it can also occur if the direction of the dipole moment is reversed upon excitation. For such a situation, a blue shift can be observed even if the magnitude of the dipole moment increases. This shift seems to be the case for **1** and **2**; the calculations predict that upon excitation to S_1, the dipole moment increases, and its direction changes by nearly 180°.

TABLE 3: The Absorption and Fluorescence Maxima and the Fluorescence Quantum Yields and Lifetimes Measured for 1 at 293 K

solvent	$\tilde{\nu}_{abs}$ [cm^{-1}][a]	$\tilde{\nu}_{flu}$ [cm^{-1}][a]	φ_{fl}[b]	τ_{fl} [ns][c]
n-hexane	27 550	26 110	0.72	1.3
acetonitrile	27 930	25 970	0.79	1.6
1-propanol	27 550	24 810	0.25	2.6 <0.1
1-butanol	27 620	24 750	0.25	2.8 <0.1
ethanol	27 780	24 810	0.25	2.6 <0.1
methanol	27 860	24 630	0.06	0.8 <0.1

[a] Accuracy: ±40 cm^{-1}. [b] ±10%. [c] Measured with a nanosecond spectrofluorometer; estimated resolution: 0.2−0.3 ns.

TABLE 4: The Absorption and Fluorescence Maxima and the Fluorescence Quantum Yields and Lifetimes Measured for 2 at 293 K

solvent	$\tilde{\nu}_{abs}$ [cm^{-1}][a]	$\tilde{\nu}_{flu}$ [cm^{-1}][a]	φ_{fl}[b]	τ_{fl} [ns][c]
n-hexane	27 550	26 110	0.40	1.4
acetonitrile	27 860	26 040	0.51	1.7
1-propanol	27 550	25 320	0.24	2.6 <0.1
1-butanol	27 550	25 320	0.26	2.5 <0.1
ethanol	27 620	25 190	0.22	2.3 <0.1
methanol	27 700	24 940	0.08	0.9 <0.1

[a] Accuracy: ±40 cm^{-1} [b] ±10%. [c] Measured with a nanosecond spectrofluorometer; estimated resolution: 0.2−0.3 ns.

The positions of the absorption and fluorescence maxima, along with the quantum yields and fluorescence lifetimes, are presented in Tables 3 and 4. In hexane and acetonitrile, both compounds reveal high emission yields. In alcohol solutions, fluorescence efficiency is significantly lower. In methanol and ethylene glycol, the main band is accompanied by a very weak, low-energy emission around 20 000 cm^{-1}. The excitation spectra, measured in the region of 43 480−25 000 cm^{-1}, coincide with the absorption.

Using absorption and fluorescence data, one can obtain changes of pK_a in the excited state from the Förster cycle[101] formula

$$\Delta pK_a = pK_a(S_1) - pK_a(S_0) \approx -0.0021*(\tilde{\nu}^a_{00} - \tilde{\nu}^b_{00})$$

where $\tilde{\nu}^a_{00}$ and $\tilde{\nu}^b_{00}$ correspond to electronic transition energies in the acid and base forms, respectively. This procedure is applied using the spectra of neutral, protonated, and deprotonated species (Figure 4), thus yielding the pK_a changes upon S_1-S_0 excitation for protonation on the pyridine nitrogen atom and for deprotonation of the NH group. The 0−0 transitions are estimated from the positions of absorption and fluorescence maxima. The same value of $\Delta pK_a(N) = +10.3$ is obtained for **1** and **2**, whereas for the deprotonation, we obtain $\Delta pK_a(NH) = -6.9$ and −6.4 for **1** and **2**, respectively. These large changes of pK_a values for both deprotonation of the NH group and protonation of the pyridine nitrogen are analogous to those previously found for related molecules and prove that, upon electronic excitation, both 2-(2′-pyridyl)benzindoles become simultaneously a stronger acid and, in particular, a much stronger base. These results explain the appearance of a second weak fluorescence band at 20 000 cm^{-1} in methanol and also in ethylene glycol, the most acidic solvents used in these studies. We assign the 20 000 cm^{-1} band to the cationic form, obtained by protonation of the chromophore in the excited electronic state. This assignment is corroborated not only by the excitation spectra corresponding to the absorption of neutral species but also by the finding that the weak emission, observed at 293 K, disappears below 143 K and reappears again with warming of the sample.

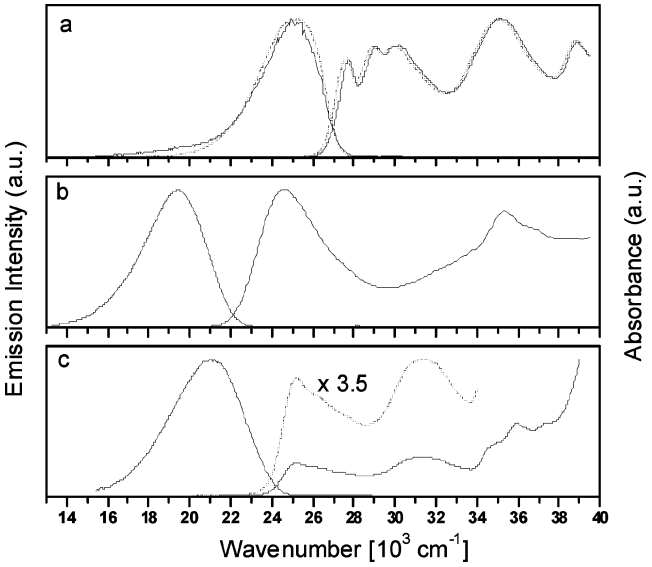

Figure 4. Room-temperature absorption and fluorescence of **2**: (a) neutral (ethanol, dashed line; methanol, solid line), (b) protonated (ethanol + $HClO_4$), and (c) deprotonated (DMSO + KOH).

The steady-state measurements did not reveal any emission that could be associated with the phototautomer. However, this observation does not necessarily prove the absence of the photoreaction since the tautomeric form can, in principle, be rapidly deactivated, or, as actually predicted by calculations (Figure 1), lie outside of the spectral range available for detection. The analysis of the fluorescence lifetimes (Tables 3 and 4) shows that while the decays are monoexponential in *n*-hexane and acetonitrile, this behavior is not the case in alcohol solutions. For the latter, biexponential decays are obtained, with one of the lifetimes about twice as long as that in *n*-hexane and acetonitrile and the other too short to be accurately measured by our subnanosecond spectrofluorometer. We therefore investigated the decays more closely by using femtosecond transient absorption and picosecond time-resolved emission techniques.

3.3. Time-Resolved Measurements. To elucidate the origin of the observed fluorescence, in particular, the complicated character of the emission in alcohols, we performed time-resolved fluorescence measurements using a picosecond time-correlated single-photon counting setup (SPC). The fluorescence decay curves were fitted to a multiexponential linear function

$$I(\lambda,t) = \sum_{i=1}^{n} a_i(\lambda) \exp\left(-\frac{t}{\tau_i}\right)$$

where $a_i(\lambda)$ are the amplitudes of different lifetimes τ_i.

The fractional contribution of each decay time component to the steady-state emission was calculated according to

$$f_i(\lambda) = \frac{a_i(\lambda)\tau_i}{\sum_j a_j(\lambda)\tau_j}$$

Next, the DAES (decay associated emission spectra) were built using DAES = $f_i(\lambda)\cdot I(\lambda)$, where $I(\lambda)$ is the steady-state emission spectrum. The spectra are presented in Figure 5.

The DAES in *n*-hexane and acetonitrile consist of only one band, decaying with the same lifetime as that obtained from standard measurements (Tables 3 and 4). On the other hand, in alcohols, the biexponential character of fluorescence decay is

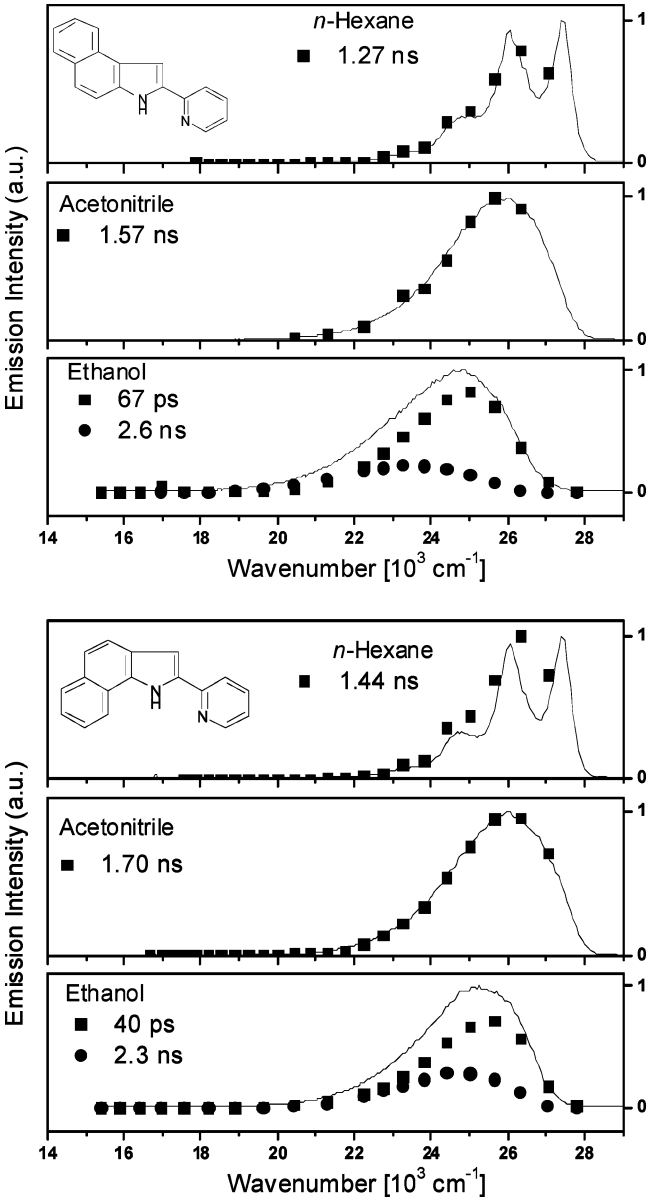

Figure 5. Decay associated emission spectra of **1** and **2** in *n*-hexane, acetonitrile, and ethanol. Solid lines are the steady-state emission spectra, and the symbols are for DAES.

confirmed. Fluorescence consists of a short-lived (tens of picoseconds) band and a long-lived emission, which decays with the same lifetime as that detected by standard SPC experiments. By analogy to previous studies,[20,32] it is natural to assign the latter to the *anti* species, whereas the short-lived component can be attributed to the *syn* forms, rapidly deactivated by either ESPT or internal conversion in complexes with alcohol.

The situation in methanol is even more complex. Triexponential functions had to be applied for the satisfactory fitting of the decay curves. One of the kinetic parameters corresponds to a rise time in the spectral region around 20 000 cm^{-1}. The fluorescence maxima of protonated and deprotonated molecules lie also in the area of 20 000 cm^{-1} (Figure 4). Time-resolved measurements for protonated and deprotonated molecules reveal that the lifetime for protonated **1** and **2** is about 1 ns, while for deprotonated forms, it is much longer (6 ns). Since the weak shoulder in the emission is observed only in methanol and ethylene glycol, the most acidic solvents in the series we investigate, but not in other protic solvents, it is natural to attribute this band to the protonated form. The rise times were

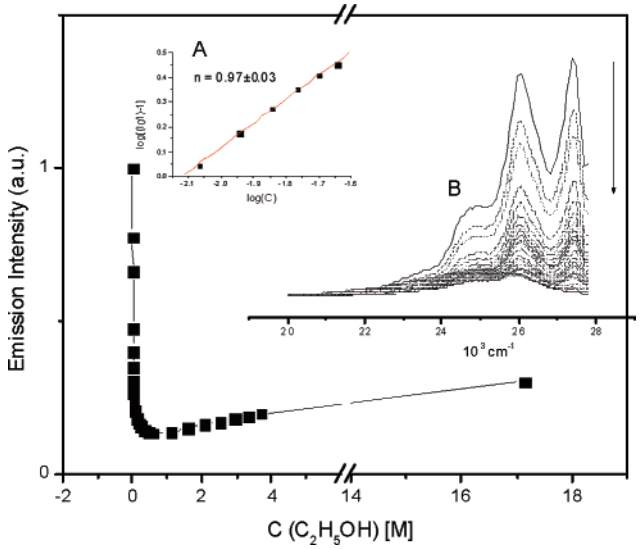

Figure 6. Spectrofluorimetric titration of **1** in *n*-hexane with ethanol at 293 K. Inset A: a plot of $\log(I_0/I - 1)$ versus the logarithm of alcohol concentration. Inset B: changes in fluorescence intensity upon adding alcohol.

detected in the DAES around 20 000 cm^{-1}, which can be attributed to the formation of the protonated species in methanol. For the solutions in ethylene glycol, the rise times increased, while in acidic solutions, they were much shorter. These components were absent in ethanol solutions, where the additional emission band around 20 000 cm^{-1} was not observed.

The most significant result of the DAES analysis is the presence in alcohols of a short-lived (e.g., 67 ps in **1** and 40 ps in **2** for ethanol) emission band, slightly blue-shifted from the main emission maximum (Figure 5). The long-lived emission in ethanol, 1-propanol, and 1-butanol decays with a lifetime nearly twice as long as that in *n*-hexane or acetonitrile. This observation indicates that the radiative constant in the long-lived form is smaller than that of the *syn* species observed in aprotic solvents. By analogy with our previous studies of similar molecules,[20,32] it is natural to assign the long-lived form to the *anti* rotamer. Assuming similar absorption coefficients for *syn* and *anti* alcohol solvates, it can be estimated that both forms exist in bulk alcohols in comparable amounts, whereas the *syn* form is predominant in aprotic media.

Regarding the nature of the short-lived species in alcohols, at least two structures have to be considered. The first is a 1:1 complex of the *syn* form with alcohol. In such a structure, ESPT is to be expected, with the barrier to tautomerization significantly lower than that in the uncomplexed species. The other candidate is the complex of 1:2 (or more generally, 1:*n*) stoichiometry, again of the *syn* type. For such a kind of species, rapid internal conversion to the ground state has been reported.[31] This process is strongly dependent on the viscosity, and thus, its rate should become slower upon passing from methanol and ethanol to more viscous alcohols. On the other hand, the ESPT reaction in 1:1 complexes should not depend strongly on viscosity. The fluorescence decay components of 67 and 40 ps in ethanol for **1** and **2**, respectively, become shorter in methanol (25 and 13 ps), whereas in ethylene glycol, they increase significantly (to 160 and 110 ps). This behavior is analogous to that observed previously for various bifunctional compounds,[22] in which the decay components ranging from 50 to 76 ps were observed in ethanol. These decays were assigned to internal conversion in 1:2 complexes with alcohol. The ESPT in 1:1 species was characterized by much shorter lifetimes (subpicoseconds to a few picoseconds). Thus, the present picosecond experiments point to the domination, in bulk alcohols, of 1:2 *syn* complexes. However, the existence of 1:1 complexes cannot be excluded. Actually, such species should prevail in mixed solvents containing small amounts of alcohol. A strong confirmation for such an assignment was provided by spectrofluorimetric titration of *n*-hexane solutions of **1** and **2** with alcohols (Figure 6). Very efficient fluorescence quenching was observed at low alcohol concentrations. The emission intensity passes through a minimum and then increases upon adding more alcohol. Such a rather unusual behavior can be explained by a scheme presented in Figure 7. Adding small amounts of alcohols to the solution containing only the *syn* species leads to the formation of 1:1 complexes, which rapidly decay via ESPT. The excess of alcohol results in *syn* → *anti* rotamerization due to the energetically more favorable linear dual hydrogen bond with two alcohol molecules in the *anti* structure. The *anti* complexes can undergo neither ESPT nor internal conversion. Therefore, they decay with a "normal" long lifetime.

The slope of the plot of $\log(I/I_0 - 1)$ versus $\log(c)$, where I_0 and I correspond to fluorescence intensities in the absence and presence of alcohol, respectively, and c is the alcohol concentration, should give n, the number of alcohol molecules involved in the complex. Such a procedure, applied to **1**, yielded $n = 0.97 \pm 0.03$, proving the existence of the 1:1 species. In bulk alcohols, the equilibrium between 1:1 and 1:2 complexes may be strongly shifted in favor of the latter. In order to find evidence for a short fluorescence decay characteristic of ESPT, and thus for the presence of 1:1 *syn* species, we performed transient absorption experiments with subpicosecond resolution.

The transient absorption spectra have been unraveled by global analysis in combination with a target analysis. These procedures yielded evolution associated difference spectra (EADS), which represent temporal evolution of the spectra (e.g., the third EAD spectrum rises with the second lifetime and decays with the third lifetime).[102]

Global analysis of the data in *n*-hexane solutions (Figures 8a−9a) reveals that they can be fitted satisfactorily with a model consisting of two components, 34 and 840 ps for **1** and 20 ps and about 1.5 ns for **2**. The pump-induced change in the absorbance has contributions from two sources, stimulated emission and excited-state absorbance. The negative-going features above 25 000 cm^{-1} correspond to the well-resolved stimulated emission. The positive-going bands near 18 000−

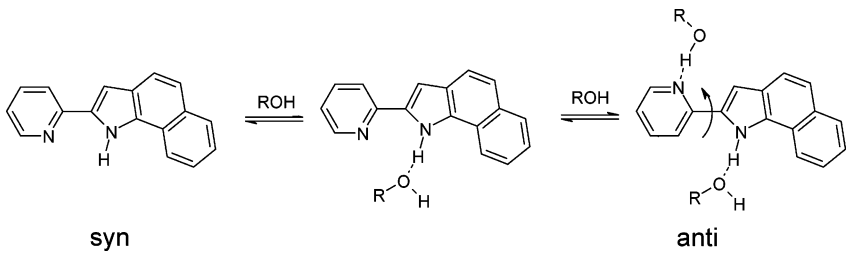

Figure 7. Scheme of protic solvation resulting in *syn*−*anti* rotamerization.

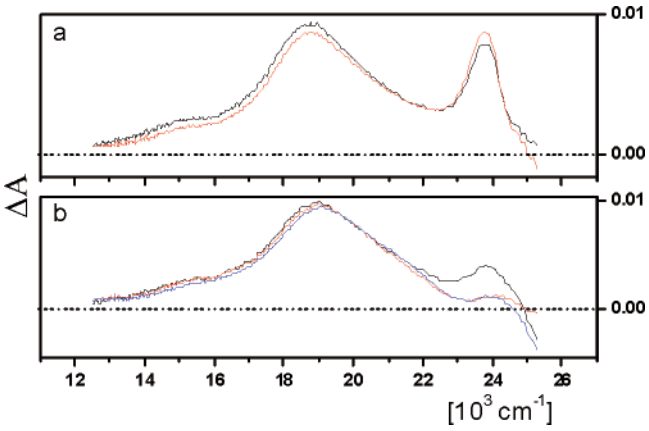

Figure 8. EADS of **1** in *n*-hexane (a) and acetonitrile (b) obtained for excitation at 360 nm. In *n*-hexane, the black and red EADS are associated with decay times of 17 ps and 1.2 ns, respectively. In acetonitrile, the black, red, and blue EADS decay with 0.8 ps, 21 ps, and 1.5 ns, respectively.

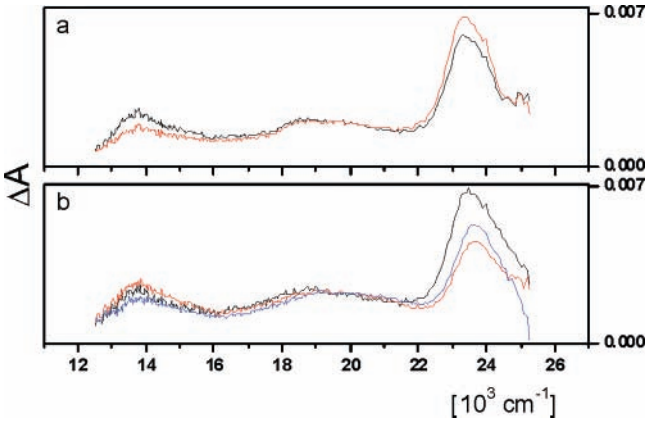

Figure 9. EADS of **2** in *n*-hexane (a) and acetonitrile (b) obtained for excitation at 360 nm. In *n*-hexane, the black and red EADS are associated with decay times of 16 ps and 2.2 ns, respectively. In acetonitrile, the black, red, and blue EADS decay with 0.5 ps, 24 ps, and 3.0 ns, respectively.

19 000 and 23 000−24 000 cm^{-1} correspond to excited-state absorbance of the "normal" *syn* form. There is not any indication for structural changes of the molecules taking place in the excited state, except vibrational cooling. Similar observations and decay times are valid also for the transient absorption spectra in *n*-dodecane, which means that there is no viscosity dependence in the relaxation mechanism. These results demonstrate again that no ESPT occurs in *n*-hexane solutions of **1** and **2**. The possibility of a rapid "over the barrier" process can also be discarded; in other words, the vibrational relaxation is faster than ESPT.

The spectra obtained in acetonitrile, a polar aprotic medium (Figures 8b−9b), resemble those measured in *n*-hexane. On the contrary, the kinetic curves recorded in alcohols reveal much more complicated dynamics (Figure 10). In particular, several short decay components (1−11ps) are detected in alcohols. They can be indicative of ESPT in 1:1 cyclic *syn* complexes. However, they can also be related to vibrational cooling or solvent relaxation times.[103] Most important, the data for alcohols show a transient absorption feature around 23 000−24 000 cm^{-1}, which decays rapidly, similarly to the short-lived band observed in fluorescence. Thus, the coexistence of two different conformers is confirmed once again. The feature around 24 000 cm^{-1} is clearly observed also in *n*-hexane and acetonitrile, where it decays slowly, similar to the overall spectrum. Since there is no doubt about the dominance of the *syn* form in *n*-hexane and acetonitrile, the fast decay of the 24 000 cm^{-1} band in alcohols proves that the same conformer also exists in alcohols, where its excited state is rapidly deactivated due to the formation of hydrogen bonds with the solvent. The fast deactivation most probably involves both ESPT and internal conversion, but the clear separation of the various factors contributing to picosecond changes in excited-state absorption is not straightforward. The detailed analysis of the kinetic behavior in alcohols will be presented elsewhere.

Summary and Conclusions

Stationary and time-resolved studies of 2-(2′-pyridyl)benzindoles in nonpolar, as well as in polar aprotic and protic media, allow us not only to make conclusions about the structure and reactivity of these two chromophores but also to understand differences and similarities in their behavior as compared with smaller, but strongly structurally related, molecules, such as **3** and **4**. The first finding is that the majority of the molecules exist in the *syn* form in aprotic solvents. In alcohols, on the contrary, *syn* and *anti* structures are detected in comparable amounts. In this respect, 2-(2′-pyridyl)benzindoles are different from the smaller members of the series, most probably because of the reduced role of nonspecific solvation (stabilization of the more polar *anti* form by a polar solvent).

The finding that *syn* structures can exist even in protic media has important consequences for the photophysics, as the ESPT reaction can occur only in this type of rotamer. It can be anticipated that further increase in the molecular size will shift the equilibrium in alcohols toward *syn* species. The possibility of totally changing the photophysical characteristics while

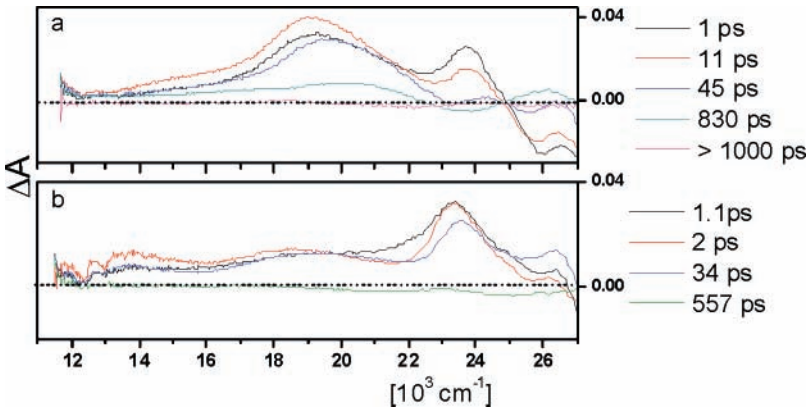

Figure 10. EADS of **1** (a) and **2** (b) in ethanol, obtained for excitation at 360 nm. The corresponding decay times are indicated on the right.

retaining the basic topological motif, the location of proton donor and acceptor sites, will be the subject of future studies. We also will carry out the comparative analysis of the electronic absorptions of **1** and **2** in different solvents in order to (i) understand substantial differences in the intensity patterns and (ii) separate spectra due to different species. Initial results obtained using magnetic circular dichroism (MCD) confirm the presence of a different structure in alcohols as compared to that in hexane, once again revealing the solvent-induced rotamerization.

The most challenging structural task is to distinguish between various types of alcohol complexes for one type of rotational conformer. While not quantitatively accurate, our data suggest that both 1:1 and 1:2 *syn* complexes are present, and the latter dominate in bulk alcohols. Comparison with previous experimental data[20,31] and MD simulations[21,79] reveals a certain trend. In the bifunctional compounds, for which the hydrogen donor and acceptor groups are linked by a single bond, the 1:2 species prevail. The opposite is true when the donor and acceptor groups are rigidly bound. Most probably, in compounds of the former class, the conformational flexibility allows for geometry distortions that can better accommodate a triple hydrogen bond structure in 1:2 complexes. Detailed studies of stoichiometry and the structure of water and alcohol solvates of bifunctional compounds are now being carried out in our laboratories for molecules isolated in supersonic jets.[86]

Acknowledgment. I.P. acknowledges the support from the EC Grant G5MA-CT-2002-04026. R.P.T., A.S., and M.S.M. thank the Robert A. Welch Foundation (E-621) and the National Science Foundation (CHE-0352617) for financial support of this work. I.P. is grateful to The Netherlands Organization for Scientific Research (NWO) for providing financial support for a long-term fellowship. The authors are very grateful to Dr. Hong Zhang for fruitful discussions and Katharine Mullen for the help in the global analysis of the transient absorption data.

References and Notes

(1) Mataga, N.; Kaibe, Y.; Koizumi, M. *Nature* **1955**, *175*, 731.
(2) Rehm, D.; Weller, A. *Isr. J. Chem.* **1970**, 259.
(3) Suter, G. W.; Wild, U. P.; Schaffner, K. *J. Phys. Chem.* **1986**, *90*, 2358.
(4) Herbich, J.; Rettig, W.; Thummel, R. P.; Waluk, J. *Chem. Phys. Lett.* **1992**, *195*, 556.
(5) Herbich, J.; Waluk, J.; Thummel, R. P.; Hung, C. Y. *J. Photochem. Photobiol., A* **1994**, *80*, 157.
(6) Mataga, N.; Miyasaka, H. *Prog. React. Kinet.* **1994**, 317.
(7) Benigno, A. J.; Ahmed, E.; Berg, M. *J. Chem. Phys.* **1996**, *104*, 7382.
(8) Herbich, J.; Hung, C. Y.; Thummel, R. P.; Waluk, J. *J. Am. Chem. Soc.* **1996**, *118*, 3508.
(9) Biczók, L.; Bérces, T.; Linschitz, H. *J. Am. Chem. Soc.* **1997**, *119*, 11071.
(10) Herbich, J.; Dobkowski, J.; Thummel, R. P.; Hegde, V.; Waluk, J. *J. Phys. Chem. A* **1997**, *101*, 5839.
(11) Yatsuhashi, T.; Inoue, H. *J. Phys. Chem. A* **1997**, *101*, 8166.
(12) Chudoba, C.; Nibbering, E. T. J.; Elsaesser, T. *Phys. Rev. Lett.* **1998**, *81*, 3010.
(13) Dobkowski, J.; Herbich, J.; Galievsky, V.; Thummel, R. P.; Wu, F. Y.; Waluk, J. *Ber. Bunsen-Ges. Phys. Chem. Chem. Phys.* **1998**, *102*, 469.
(14) Yatsuhashi, T.; Nakajima, Y.; Shimada, T.; Inoue, H. *J. Phys. Chem. A* **1998**, *102*, 3018.
(15) Biczók, L.; Bérces, T.; Inoue, H. *J. Phys. Chem. A* **1999**, *103*, 3837.
(16) Biczók, L.; Valat, P.; Wintgens, V. *Phys. Chem. Chem. Phys.* **1999**, *1*, 4759.
(17) Chudoba, C.; Nibbering, E. T. J.; Elsaesser, T. *J. Phys. Chem. A* **1999**, *103*, 5625.
(18) Kyrychenko, A.; Herbich, J.; Izydorzak, M.; Gil, M.; Dobkowski, J.; Wu, F. Y.; Thummel, R. P.; Waluk, J. *Isr. J. Chem.* **1999**, *39*, 309.
(19) Kyrychenko, A.; Herbich, J.; Izydorzak, M.; Wu, F.; Thummel, R. P.; Waluk, J. *J. Am. Chem. Soc.* **1999**, *121*, 11179.
(20) Kyrychenko, A.; Herbich, J.; Wu, F.; Thummel, R. P.; Waluk, J. *J. Am. Chem. Soc.* **2000**, *122*, 2818.
(21) Kyrychenko, A.; Stepanenko, Y.; Waluk, J. *J. Phys. Chem. A* **2000**, *104*, 9542.
(22) Marks, D.; Zhang, H.; Borowicz, P.; Waluk, J.; Glasbeek, M. *J. Phys. Chem. A* **2000**, *104*, 7167.
(23) Singh, A. K.; Bhasikuttan, A. C.; Palit, D. K.; Mittal, J. P. *J. Phys. Chem. A* **2000**, *104*, 7002.
(24) Waluk, J. In *Conformational analysis of Molecules in Excited States*; Waluk, J., Ed.; Wiley-VCH: New York, 2000; p 57.
(25) Herbich, J.; Kijak, M.; Luboradzki, R.; Gil, M.; Zielińska, A.; Hu, Y. Z.; Thummel, R. P.; Waluk, J. *J. Photochem. Photobiol., A* **2002**, *154*, 61.
(26) Herbich, J.; Kijak, M.; Zielińska, A.; Thummel, R. P.; Waluk, J. *J. Phys. Chem. A* **2002**, *106*, 2158.
(27) Kijak, M.; Zielińska, A.; Thummel, R. P.; Herbich, J.; Waluk, J. *Chem. Phys. Lett.* **2002**, *366*, 329.
(28) Józefowicz, M.; Heldt, J. R. *Chem. Phys.* **2003**, *294*, 105.
(29) Kwok, W. M.; George, M. W.; Grills, D. C.; Ma, C. S.; Matousek, P.; Parker, A. W.; Phillips, D.; Toner, W. T.; Towrie, M. *Angew. Chem., Int. Ed.* **2003**, *42*, 1826.
(30) Palit, D. K.; Zhang, T. Q.; Kumazaki, S.; Yoshihara, K. *J. Phys. Chem. A* **2003**, *107*, 10798.
(31) Waluk, J. *Acc. Chem. Res.* **2003**, *36*, 832.
(32) Kijak, M.; Zielińska, A.; Chamchoumis, C.; Herbich, J.; Thummel, R. P.; Waluk, J. *Chem. Phys. Lett.* **2004**, *400*, 279.
(33) Sebök-Nagy, K.; Biczók, L. *Photochem. Photobiol. Sci.* **2004**, *3*, 389.
(34) Sebök-Nagy, K.; Biczók, L.; Morimoto, A.; Shimada, T.; Inoue, H. *Photochem. Photobiol.* **2004**, *80*, 119.
(35) Wiosna, G.; Petkova, I.; Mudadu, M. S.; Thummel, R. P.; Waluk, J. *Chem. Phys. Lett.* **2004**, *400*, 379.
(36) Samant, V.; Singh, A. K.; Ramakrishna, G.; Ghosh, H. N.; Ghanty, T. K.; Palit, D. K. *J. Phys. Chem. A* **2005**, *109*, 8693.
(37) Arnaut, L. G.; Formosinho, S. J. *J. Photochem. Photobiol., A* **1993**, *75*, 1.
(38) Formosinho, S. J.; Arnaut, L. G. *J. Photochem. Photobiol., A* **1993**, *75*, 21.
(39) Ormson, S. M.; Brown, R. G. *Prog. React. Kinet.* **1994**, *19*, 45.
(40) Saenger, W. *Principles of Nucleic acid Structures*; Springer-Verlag: New York, 1984.
(41) Strazewski, P.; Tamm, C. *Angew. Chem., Int. Ed. Engl.* **1990**, *26*, 36.
(42) Taylor, C. A.; El-Bayoumi, M. A.; Kasha, M. *Proc. Natl. Acad. Sci. U.S.A.* **1969**, *63*, 253.
(43) Ingham, K. C.; El-Bayoumi, M. A. *J. Am. Chem. Soc.* **1974**, *96*, 1674.
(44) Bulska, H.; Grabowska, A.; Pakuła, B.; Sepioł, J.; Waluk, J. *J. Lumin.* **1984**, *29*, 65.
(45) Fuke, K.; Yoshiuchi, H.; Kaya, K. *J. Phys. Chem.* **1984**, *88*, 5840.
(46) Fuke, K.; Kaya, K. *J. Phys. Chem.* **1989**, *93*, 614.
(47) Share, P.; Pereira, M.; Sarisky, M. *J. Lumin.* **1991**, *48/49*, 204.
(48) Douhal, A.; Kim, S. K.; Zewail, A. H. *Nature* **1995**, *378*, 260.
(49) LopezMartens, R.; Long, P.; Solgadi, D.; Soep, B.; Syage, J.; Millie, P. *Chem. Phys. Lett.* **1997**, *273*, 219.
(50) Takeuchi, S.; Tahara, T. *Chem. Phys. Lett.* **1997**, *277*, 340.
(51) Takeuchi, S.; Tahara, T. *J. Phys. Chem. A* **1998**, *102*, 7740.
(52) Chachisvilis, M.; Fiebig, T.; Douhal, A.; Zewail, A. H. *J. Phys. Chem. A* **1998**, *102*, 669.
(53) Folmer, D. E.; Poth, L.; Wisniewski, E. S.; Castleman, A. W. *Chem. Phys. Lett.* **1998**, *287*, 1.
(54) Folmer, D. E.; Wisniewski, E. S.; Hurley, S. M.; Castleman, A. W. *Proc. Natl. Acad. Sci. U.S.A.* **1999**, *96*, 12980.
(55) Fiebig, T.; Chachisvilis, M.; Manger, M.; Zewail, A. H.; Douhal, A.; Garcia-Ochoa, I.; Ayuso, A. D. H. *J. Phys. Chem. A* **1999**, *103*, 7419.
(56) Catalán, J.; del Valle, J. C.; Kasha, M. *Proc. Natl. Acad. Sci. U.S.A.* **1999**, *96*, 8338.
(57) Guallar, V.; Batista, V. S.; Miller, W. H. *J. Chem. Phys.* **1999**, *110*, 9922.
(58) Catalán, J.; del Valle, J. C.; Kasha, M. *Chem. Phys. Lett.* **2000**, *318*, 629.
(59) Folmer, D. E.; Wisniewski, E. S.; Castleman, A. W. *Chem. Phys. Lett.* **2000**, *318*, 637.
(60) Douhal, A.; Moreno, M.; Lluch, J. M. *Chem. Phys. Lett.* **2000**, *324*, 81.
(61) Catalán, J.; Kasha, M. *J. Phys. Chem. A* **2000**, *104*, 10812.
(62) Takeuchi, S.; Tahara, T. *Chem. Phys. Lett.* **2001**, *347*, 108.
(63) Catalán, J.; Perez, P.; del Valle, J. C.; de Paz, J. L. G.; Kasha, M. *Proc. Natl. Acad. Sci. U.S.A.* **2002**, *99*, 5793.
(64) Catalán, J.; Perez, P.; del Valle, J. C.; de Paz, J. L. G.; Kasha, M. *Proc. Natl. Acad. Sci. U.S.A.* **2002**, *99*, 5799.
(65) Catalán, J.; Perez, P.; Del Valle, J. C.; De Paz, J. L. G.; Kasha, M. *Proc. Natl. Acad. Sci. U.S.A.* **2004**, *101*, 419.

(66) Catalán, J.; de Paz, J. L. G. *J. Chem. Phys.* **2005**, *123*, 114302.
(67) Sakota, K.; Sekiya, H. *J. Phys. Chem. A* **2005**, *109*, 2718.
(68) Sakota, K.; Sekiya, H. *J. Phys. Chem. A* **2005**, *109*, 2722.
(69) Sakota, K.; Okabe, C.; Nishi, N.; Sekiya, H. *J. Phys. Chem. A* **2005**, *109*, 5245.
(70) Avouris, A.; Yang, L. L.; El-Bayoumi, M. A. *Photochem. Photobiol.* **1976**, *24*, 211.
(71) Konijnenberg, J.; Huizer, A. H.; Varma, C. *J. Chem. Soc., Faraday Trans. 2* **1988**, *84*, 1163.
(72) McMorrow, D.; Aartsma, T. *Chem. Phys. Lett.* **1986**, *125*, 581.
(73) Moog, R. S.; Bovino, S. C.; Simon, J. D. *J. Phys. Chem.* **1988**, *92*, 6545.
(74) Chou, P. T.; Martinez, M. L.; Cooper, W. C.; McMorrow, D.; Collins, S. T.; Kasha, M. *J. Phys. Chem.* **1992**, *96*, 5203.
(75) Chapman, C. F.; Maroncelli, M. *J. Phys. Chem.* **1992**, *96*, 8430.
(76) Chen, Y.; Gai, F.; Petrich, J. W. *J. Am. Chem. Soc.* **1993**, *115*, 10158.
(77) Chen, Y.; Gai, F.; Petrich, J. W. *Chem. Phys. Lett.* **1994**, *222*, 329.
(78) Smirnov, A. V.; English, D. S.; Rich, R. L.; Lane, J.; Teyton, L.; Schwabacher, A. W.; Luo, S.; Thornburg, R. W.; Petrich, J. W. *J. Phys. Chem. B* **1997**, *101*, 2758.
(79) Mente, S.; Maroncelli, M. *J. Phys. Chem. A* **1998**, *102*, 3860.
(80) Folmer, D. E.; Wisniewski, E. S.; Stairs, J. R.; Castleman, A. W. *J. Phys. Chem. A* **2000**, *104*, 10545.
(81) Fernández-Ramos, A.; Smedarchina, Z.; Siebrand, W.; Zgierski, M. Z. *J. Chem. Phys.* **2001**, *114*, 7518.
(82) Kwon, O. H.; Lee, Y. S.; Park, H. J.; Kim, Y.; Jang, D. J. *Angew. Chem., Int. Ed.* **2004**, *43*, 5792.
(83) Hara, A.; Sakota, K.; Nakagaki, M.; Sekiya, H. *Chem. Phys. Lett.* **2005**, *407*, 30.
(84) Kwon, O. H.; Jang, D. J. *J. Phys. Chem. B* **2005**, *109*, 8049.
(85) Kijak, M.; Nosenko, E.; Singh, A.; Thummel, R. P.; Waluk, J. *J. Am. Chem. Soc.* **2007**, *129*, 2738.
(86) Nosenko, Y.; Kunitski, M.; Thummel, R. P.; Kyrychenko, A.; Herbich, J.; Waluk, J.; Riehn, C.; Brutschy, B. *J. Am. Chem. Soc.* **2006**, *128*, 10000.
(87) Robinson, B. *The Fisher Indole Synthesis*; Wiley: New York, 1982.
(88) Velapoldi, R. A. *Accuracy in Spectrophotometry and Luminescence Measurements*, Proceedings of the Conference of the National Bureau of Standards, National Bureau of Standards Special Publication 378; National Nureau of Standards: Gaithersburg, MD, 1972; p 231.
(89) Van Dijk, S. I.; Wiering, P. G.; Groen, C. P.; Brouwer, A. M.; Verhoeven, J. W.; Schuddeboom, W.; Warman, J. M. *J. Chem. Soc., Faraday Trans.* **1996**, *91*, 2107.
(90) Balkowski, G.; Szemik-Hojniak, A.; van Stokkum, I. H. M.; Zhang, H.; Buma, W. J. *J. Phys. Chem. A.* **2005**, *109*, 3535.
(91) Treutler, O.; Ahlrichs, R. *J. Chem. Phys.* **1995**, *102*, 346.
(92) Von Arnim, M.; Ahlrichs, R. *J. Comput. Chem.* **1998**, *19*, 1746.
(93) Deglmann, P.; Furche, F.; Ahlrichs, R. *Chem. Phys. Lett.* **2002**, *362*, 511.
(94) Deglmann, P.; Furche, F. *J. Chem. Phys.* **2002**, 9535.
(95) Schäfer, A.; Huber, C.; Ahlrichs, R. *J. Chem. Phys.* **1994**, *100*, 5829.
(96) Becke, D. *J. Chem. Phys.* **1993**, 5648.
(97) Lee, C.; Yang, W.; Parr, R. G. *Phys. Rev. B* **1988**, *37*, 785.
(98) Furche, F.; Ahlrichs, R. *J. Chem. Phys.* **2002**, *117*, 7433.
(99) Kyrychenko, A.; Waluk, J. *J. Phys. Chem. A* **2006**, *110*, 11958.
(100) Kijak, M.; Buma, W. J.; Waluk, J. In preparation.
(101) Förster, T. *Z. Elektrochem.* **1950**, 42.
(102) van Stokkum, I. H. M.; Larsen, D. S.; van Grondelle, R. *Biochim. Biophys. Acta* **2004**, *1657*, 82; *1658*, 262 (erratum).
(103) Horng, M. L.; Gardecki, J. A.; Papazyan, A.; Maroncelli, M. *J. Phys. Chem.* **1995**, *99*, 17311.